THE JOURNAL OF BIOLOGICAL CHEMISTRY VOL. 281, NO. 42, pp. 31677–31688, October 20, 2006

Identification of a Tyrosine-based Motif (YGSI) in the Amino Terminus of Nramp1 (Slc11a1) That Is Important for Lysosomal Targeting*[S]

Received for publication, February 27, 2006, and in revised form, July 25, 2006 Published, JBC Papers in Press, August 12, 2006, DOI 10.1074/jbc.M601828200

Steven Lam-Yuk-Tseung, Virginie Picard, and Philippe Gros[1]

From the Department of Biochemistry, McGill Cancer Center and Center for Host Resistance, McGill University, Montreal, Quebec H3G 1Y6, Canada

In macrophages, *Nramp1* (*Slc11a1*) is expressed in lysosomes and restricts replication of intracellular pathogens by removing divalent metals (Mn^{2+} and Fe^{2+}) from the phagolysosome. *Nramp2* (*DMT1*, *Slc11a2*) is expressed both at the duodenal brush border where it mediates uptake of dietary iron and ubiquitously at the plasma membrane/recycling endosomes of many cell types where it transports transferrin-associated iron across the endosomal membrane. In Nramp2, a carboxyl-terminal cytoplasmic motif (^{555}YLLNT^{559}) is critical for internalization and recycling of the transporter from the plasma membrane. Here we studied the subcellular trafficking properties of Nramp1 and investigated the *cis*-acting sequences responsible for targeting to lysosomes. For this, we constructed and studied Nramp1/Nramp2 chimeric proteins where homologous domains of each protein were exchanged. Chimeras exchanging the amino- (upstream TM1) and carboxyl-terminal (downstream TM12) cytoplasmic segments of both transporters were stably expressed in porcine LLC-PK_1 kidney cells and were studied with respect to expression, maturation, stability, cell surface targeting, transport activity, and subcellular localization. An Nramp2 isoform II chimera bearing the amino terminus of Nramp1 was not expressed at the cell surface but was targeted to lysosomes. This lysosomal targeting was abolished by single alanine substitutions at Tyr^{15} and Ile^{18} of a ^{15}YGSI^{18} motif present in the amino terminus of Nramp1. These results identify YGSI as a tyrosine-based sorting signal responsible for lysosomal targeting of Nramp1.

Nramp defines a large, highly conserved family of integral membrane proteins that transport divalent metals in a pH-dependent fashion (1). The first member of this family, *Nramp1* (*Slc11a1*), was identified by positional cloning of a locus (*Bcg*/*Ity*/*Lsh*) that regulates susceptibility of mice to infection with a number of unrelated intracellular pathogens (2). Naturally occurring ($Nramp1^{G169D}$) or experimentally induced ($Nramp1^{-/-}$) loss-of-function mutations at *Nramp1* cause susceptibility to infection with several species of *Mycobacterium*, *Salmonella*, and *Leishmania* (3, 4). Polymorphic variations at human *NRAMP1* have also been linked to increased susceptibility to tuberculosis and leprosy in areas where those diseases are the most prevalent (5–7). Hydropathy profiling and topological studies suggest that Nramp1 is composed of 12 putative transmembrane domains and is expressed primarily in lysosomes of mononuclear phagocytes and in tertiary granules of polymorphonuclear leukocytes (1). Upon phagocytosis of inert particles or of live pathogens, Nramp1 is rapidly recruited to the membrane of maturing phagosomes (8–11). Recent work has shown that Nramp1 functions as a phagosomal metal efflux pump that transports divalent cations such as Mn^{2+} and Fe^{2+} in a pH-dependent manner down a proton gradient created by the vacuolar H^+-ATPase (12–14). Nramp1-mediated exclusion of essential metals may impair microbial metabolic activity including expression of intracellular survival mechanisms or may directly enhance the efficacy of bactericidal effector mechanisms or both.

Nramp2 (also known as *DMT1* and *Slc11a2*) is a close homolog of *Nramp1* (15, 16) with 66% amino acid sequence identity and 77% similarity between the two proteins (17). Nramp2 is expressed abundantly and in an iron-regulated fashion at the brush border of the duodenum (18) where it imports dietary iron across the absorptive epithelium. Nramp2 is also expressed in many cell types and is abundant in erythroid precursors (19) where it is required for recruitment of transferrin-associated iron from recycling endosomes into the cytosol (20). Expression of Nramp2 has also been detected at the brush border of epithelial cells lining the proximal tubules of the kidney where it may function as a reuptake system for divalent metals (21). Two major Nramp2 protein isoforms generated by alternative splicing at 3′ exons have been identified. Isoform I (+IRE) has an iron-responsive element (IRE)[2] in the 3′-untranslated region, whereas isoform II (−IRE) lacks the IRE. In addition, the carboxyl-terminal 18 amino acids of isoform I are replaced by an alternate 25-amino acid segment in isoform II. Nramp2 isoform I is predominantly expressed in epithelial cells, whereas isoform II is predominantly expressed in erythroid cells. Much of our knowledge of the function of Nramp2 *in vivo* comes from stud-

* The costs of publication of this article were defrayed in part by the payment of page charges. This article must therefore be hereby marked "*advertisement*" in accordance with 18 U.S.C. Section 1734 solely to indicate this fact.

[S] The on-line version of this article (available at http://www.jbc.org) contains supplemental Table 1 and Figs. 1–3.

[1] To whom correspondence should be addressed: Dept. of Biochemistry, McGill University, 3655 Promenade Sir William Osler, Montreal, Quebec H3G 1Y6, Canada. Tel.: 514-398-7291; Fax: 514-398-2603; E-mail: philippe.gros@mcgill.ca.

[2] The abbreviations used are: IRE, iron-responsive element; HA, hemagglutinin; Ab, antibody; GFP, green fluorescent protein; PBS, phosphate-buffered saline; WT, wild-type; ER, endoplasmic reticulum; NT, amino-terminal; AP, adaptor protein.

ies of rodent models of microcytic anemia and iron deficiency including the *mk* mouse and the Belgrade rat, that are both caused by the same missense mutation in predicted TM4 of Nramp2 (G185R) (22, 23). This phenotype is recapitulated in a mouse mutant with targeted inactivation of *Nramp2* (*Nramp2*$^{-/-}$) (24). Recently two human patients with severe hypochromic microcytic anemia and hepatic iron overload were shown to harbor mutations in *NRAMP2* (25, 26). In both patients, a quantitative reduction in the expression of functional *Nramp2* has been identified as the cause of disease (27–29).

Although *Nramp1* and *Nramp2* code for functionally undistinguishable pH-dependent divalent metal transporters with similar substrate specificities (13), they differ sharply in their subcellular localizations. Nramp1 is found strictly at the lysosomal compartment of cells with no expression at the cell surface (8, 9). In contrast, Nramp2 is ubiquitously expressed at the plasma membrane as well as in recycling endosomes (isoform II) at steady state (18, 30). Sequence motifs found in the cytoplasmic terminal regions of membrane proteins often control their subcellular targeting and trafficking (31, 32). The most common motifs are either tyrosine-based signals of the forms NP*X*Y or Y*XX*Φ (where *X* = any residue, and Φ = large hydrophobic residues) and dileucine-based motifs (LL) (33). The subcellular trafficking of Nramp1 is not well understood, and specific cytoplasmic motifs involved in its lysosomal targeting have not yet been identified. However, we have shown previously that insertion of a hemagglutinin (HA) epitope tag in the fourth extracytoplasmic loop of Nramp1 causes the transporter to be mistargeted to the plasma membrane where it displays metal uptake activity (13). On the other hand, trafficking signals in the amino and carboxyl cytoplasmic regions of Nramp2 have been identified and characterized. We and others have shown that a ^{555}YLLNT^{559} motif in the carboxyl terminus of Nramp2 isoform II controls targeting to transferrin-positive recycling endosomes (31, 32). Deletion of this motif or truncation of the entire carboxyl-terminal cytoplasmic segment of Nramp2 isoform II results in a mutant protein that is internalized less rapidly from the plasma membrane, is not properly recycled back to the cell surface, and is targeted to late endosomes and lysosomes (32). Mutagenesis experiments have also shown that motifs in the amino terminus of Nramp2 (NPAY and YSCF) play an additional but less determinant role in the recycling endosome targeting of Nramp2 (32).

In this study, we investigated the subcellular targeting and trafficking properties of Nramp1. For this, we constructed chimeric proteins by exchanging homologous segments of Nramp1 and Nramp2 (isoform II). We expressed the chimeras in stably transfected LLC-PK$_1$ cells and studied their expression, stability, cell surface expression, metal transport activity, and subcellular localization. We demonstrate that a tyrosine-based sorting signal of the form Y*XX*Φ functions as a lysosomal targeting motif in the amino terminus of Nramp1.

EXPERIMENTAL PROCEDURES

Materials and Antibodies—Reagent-grade chemicals were purchased from Sigma unless otherwise indicated. Monoclonal mouse antibody (Ab) HA.11 directed against the influenza HA epitope was purchased from Covance (Princeton, NJ). Cy3-labeled goat anti-rabbit and horseradish peroxidase-coupled donkey anti-mouse Abs were purchased from Jackson Immunoresearch Laboratories (West Grove, PA). Plasmids encoding GFP fusion proteins were kind gifts from Dr. D. Williams (Department of Biochemistry, University of Toronto; GFP-syntaxin 13) and Dr. Patrice Boquet (INSERM, France; GFP-Lamp1). The generation of polyclonal antibodies recognizing the amino-terminal segments of murine Nramp1 and Nramp2 proteins has been described previously (8, 30).

Plasmids and Constructs—The construction of mammalian expression plasmids containing full-length murine cDNAs for either *Nramp1* (N1/pCB6) or *Nramp2* isoform II (N2/pCB6) were described earlier (34). Full-length murine *Nramp2* cDNA (N2HA/pCB6) was modified by the in-frame addition of an exofacial HA epitope (YPYDVPDYAS) in the fourth predicted extracellular loop as described previously (34). A recombinant PCR protocol was used to generate *Nramp2-HA* chimeras bearing the amino- (N1N-HA) or carboxyl-terminal (N1C-HA) segments of *Nramp1*. Similarly *Nramp1* chimeras bearing the amino- (N2N) or carboxyl-terminal (N2C) segments of *Nramp2* were created. For *N1N-HA* and *N2N* constructs, a silent BstBI restriction enzyme site was introduced into N2HA/pCB6 and N1/pCB6 plasmids (at nucleotide positions 200 and 155, respectively) immediately preceding the first predicted transmembrane domain of each protein using primers N2-BstBI and N1-BstBI (supplemental Table 1). N1N-HA/pCB6 and N2N/pCB6 constructs were then created by exchanging XhoI-BstBI fragments of N2HA/pCB6 and N1/pCB6 plasmids. N1C-HA and N2C constructs were created by a recombinant PCR amplification protocol using chimeric oligonucleotides N2HA-N1C and N1-N2C (supplemental Table 1) showing complementarity with N1 and N2 at the boundaries of regions to be exchanged. The N2HA-N1C amplification product was inserted into N2HA/pCB6 using restriction enzyme sites SacI and EcoRI to generate N1C/pCB6. The *N1-N2C* amplification product was inserted into N1/pCB6 using restriction sites AvrII and EcoRI to generate N2C/pCB6. Alanine substitution mutations at the ^{15}YGSI^{18} motif of Nramp1 were created using mutagenic primers listed in supplemental Table 1. Mutants were introduced into N1N-HA/pCB6 using restriction enzyme sites XhoI and BstBI. The integrity of all mutant and chimeric cDNAs was verified by DNA sequencing.

Cell Culture, Transfection, and Immunoblotting—LLC-PK$_1$ cells were cultured as described previously (32) and transfected with either N1/pCB6, N2HA/pCB6, or chimeric plasmids using Lipofectamine 2000 (Invitrogen) according to instructions from the manufacturer. Stably transfected cell clones were obtained after 14 days of selection in medium containing G418 (1.4 mg/ml; Invitrogen), and individual colonies were subsequently picked and expanded. Total cell lysates were prepared and resolved by SDS-PAGE. Clones showing robust expression of the transfected constructs were identified by immunoblotting with either a mouse anti-HA Ab (for N2HA/pCB6, N1N-HA/pCB6, and N1C-HA/pCB6), a rabbit anti-Nramp2 NT Ab (N2N/pCB6), or a rabbit anti-Nramp1 NT Ab (N1/pCB6 and N2C/pCB6) as described previously (32). For experiments with cycloheximide, cells were incubated in growth medium supple-

mented with 20 μg/ml cycloheximide for the indicated time intervals prior to lysis and SDS-PAGE.

Metal Transport Assay—Measurement of metal transport in transfected LLC-PK_1 cells was carried out using a calcein fluorescence quenching assay as we have described previously (34, 35). Calcein acetoxymethyl ester (Molecular Probes) stock solutions were prepared in dimethyl sulfoxide, and cells were loaded at a final concentration of 0.25 μM calcein acetoxymethyl ester. Co^{2+} solution (2 mM cobalt chloride) was prepared fresh in deionized water. Initial rates of metal transport were calculated from the initial fluorescence quenching curves (34, 35).

Cell Surface Biotinylation—LLC-PK_1 cell monolayers were rinsed twice with ice-cold phosphate-buffered saline (PBS) and once with ice-cold borate buffer (10.0 mM boric acid, 154 mM NaCl, 7.2 mM KCl, 1.8 mM $CaCl_2$, pH 9.0) and then incubated (60 min at 4 °C) in the same buffer containing sulfo-NHS-SS-biotin (1 mg/ml; NHS is *N*-hydroxysulfosuccinimide; Pierce). Unreacted biotin was removed by three washes with RPMI 1640 medium. Biotinylated cells were collected and solubilized in lysis buffer (1% Triton X-100, 0.2% SDS, 50 mM Tris-HCl, pH 7.4, 150 mM NaCl, 20% glycerol) with protease inhibitors. Lysates were precleared by centrifugation (10,000 × *g* for 30 min at 4 °C), and protein yield was quantified by Bradford assay (Bio-Rad). Biotinylated proteins (100 μg of total protein lysate) were isolated by overnight incubation at 4 °C with 50 μl of ImmunoPure immobilized streptavidin slurry (Pierce) in a final volume of 1 ml in lysis buffer. Streptavidin beads were washed six times with cold lysis buffer, and bound proteins were eluted with 2× Laemmli buffer at room temperature for 30 min. Proteins were separated by SDS-PAGE followed by immunoblotting.

Quantification of Cell Surface Expression by Enzyme-linked Immunosorbent Assay—Quantification of Nramp2-HA molecules expressed at the cell surface by enzyme-linked immunosorbent assay was as described previously (32). Briefly LLC-PK_1 cells were grown to confluency in 48-well culture plates and fixed with 4% paraformaldehyde for 30 min. Cells were blocked in 5% nonfat milk in PBS for 30 min, incubated with anti-HA Ab (1:500) for 90 min, washed, and incubated with secondary Ab (donkey anti-mouse-horseradish peroxidase Ab, 1:4000) for 1 h. For quantification of total Nramp2-HA expression, cells were permeabilized by incubation with 0.1% Triton X-100 in PBS for 30 min prior to incubation with anti-HA Ab. Peroxidase activity was detected by incubating cells with horseradish peroxidase substrate (0.4 mg/ml *o*-phenylenediamine dihydrochloride, Sigma FAST OPD) according to the instructions from the manufacturer. Reactions were stopped after 30 min with 3 M HCl, and absorbance readings (492 nm) were taken with a spectrometer. For all determinations, background absorbance readings from (i) nonspecific binding of secondary Ab and (ii) nonspecific binding of primary Ab to vector-transfected cells were subtracted for each sample. Cell surface readings were normalized to total Nramp2-HA values for each cell clone and were expressed as a percentage.

Immunofluorescence—LLC-PK_1 cells stably expressing Nramp1, Nramp2-HA, or chimeric proteins were transiently transfected with GFP fusion proteins to label recycling endosomes (GFP-syntaxin 13) or late endosomes and lysosomes (GFP-Lamp1). Twenty-four hours later, cells were fixed with 4% paraformaldehyde (in PBS) for 20 min and were blocked and permeabilized with a PBS buffer containing 0.2% saponin and 5% nonfat milk (30 min). All antibodies were diluted in blocking solution, and incubations were performed for 1 h at room temperature. Cells stably expressing N2HA, N2N, and N1C-HA proteins were labeled with anti-Nramp2 NT Ab (1:200), whereas cells expressing N1, N1N-HA, and N2C proteins were labeled anti-Nramp1 NT Ab (1:400). All cells were subsequently incubated with a goat anti-rabbit secondary Ab coupled to Cy3. Cells were visualized using an Axiovert 200M epifluorescence microscope with a 100× oil immersion objective. Digital images were acquired with a Zeiss AxioCam HRm camera operated with AxioVision 4.3. Images were cropped, assembled, and labeled using Adobe Photoshop and Illustrator softwares.

RESULTS

Construction and Expression of Nramp1 and Nramp2 Chimeric Proteins—To better understand the trafficking of Nramp proteins, we created chimeric molecules by exchanging the predicted cytosolic amino- and carboxyl-terminal segments of Nramp1 and Nramp2. Nramp2 chimeras containing either the amino (N1N-HA) or carboxyl (N1C-HA) predicted cytosolic segments of Nramp1 were constructed using the Nramp2 isoform II (non-IRE) backbone bearing an exofacial HA tag that allowed for recognition of cell surface molecules in intact cells (Fig. 1*B*). We have shown previously that insertion of this HA tag in the fourth predicted extracytoplasmic loop (EC4) of Nramp2 (Nramp2-HA) does not affect expression, activity, subcellular localization, or recycling properties compared with the unmodified protein (36). Nramp2-HA has been used extensively to characterize the structure, function, and subcellular trafficking of this protein in LLC-PK_1 cells (27, 32, 34, 36–39). Nramp1 chimeras containing either the amino (N2N) or carboxyl (N2C) predicted cytosolic segments of Nramp2 isoform II (non-IRE) were introduced into an unmodified Nramp1 protein backbone (Fig. 1*B*). We have shown previously that an Nramp1 molecule modified by insertion of an HA tag in EC4 is mistargeted to the plasma membrane of transfected Chinese hamster ovary cells (13), precluding the use of that site for epitope tag insertion for the present studies. All Nramp1 and Nramp2 chimeras were introduced into LLC-PK_1 porcine kidney cells, and cell clones stably expressing individual variants were selected and expanded for analysis. Fig. 2*A* shows a typical immunoblot of extracts prepared from cells transfected with either *Nramp2*, *Nramp1*, or chimeric cDNAs. Immunoblots were probed separately with antibodies against the HA tag, the amino terminus of Nramp2, and the amino terminus of Nramp1. Wild-type (WT) Nramp2 was detected as two immunoreactive species, a minor species at ~60 kDa and a major species at ~90–105 kDa (Fig. 2*A*). Previous studies from our group have shown that the minor species corresponds to the precursor "core glycosylated" protein, whereas the major species corresponds to the mature "complex glycosylated" forms of the protein (36). Interestingly N1N-HA was detected as two species of faster electrophoretic mobility than WT Nramp2,

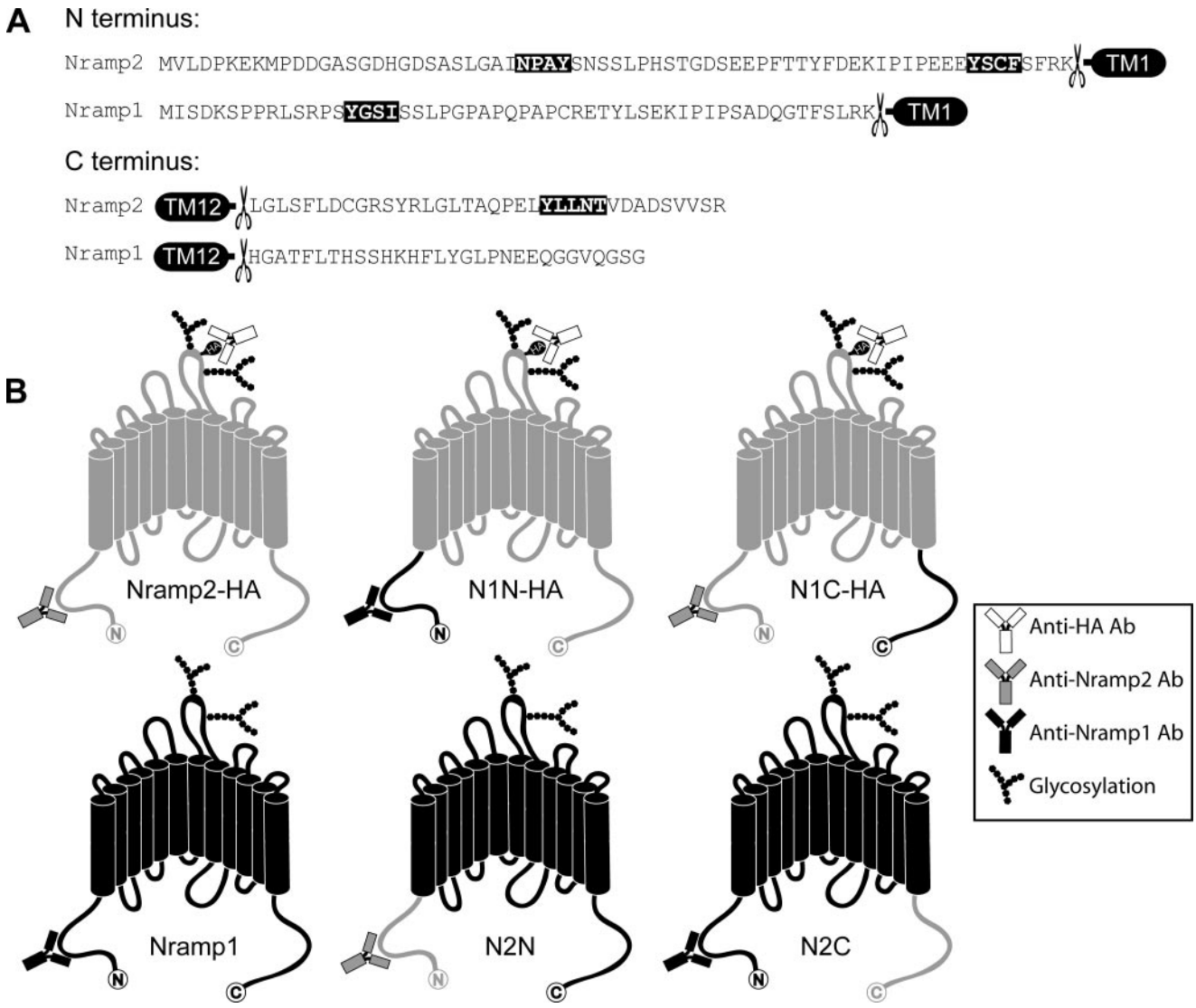

FIGURE 1. **Predicted trafficking motifs and design of Nramp1/Nramp2 chimeric proteins.** *A*, sequences of the amino- and carboxyl-terminal regions of Nramp1 and Nramp2 are shown, including the locations of predicted targeting motifs (highlighted *black*), transmembrane domains 1 (*TM1*) and 12 (*TM12*), and the locations of the sequence boundaries for the chimeras (*scissors*). In Nramp1, amino acid residues 1–54 and 519–548 were considered as the amino- and carboxyl-terminal regions, respectively. In Nramp2, residues 1–69 and 533–568 were considered as the amino- and carboxyl-terminal regions, respectively. *B*, Nramp1/2 chimeras were created by exchanging the amino- and carboxyl-terminal segments of Nramp1 and Nramp2. Schematic representations are shown of wild-type Nramp2-HA (*gray*) and wild-type Nramp1 (*black*) as well as the four chimeras created. The positions of antigenic epitopes recognized by the anti-HA, anti-Nramp1, and anti-Nramp2 antibodies as well as the putative *N*-linked glycosylation sites (Nramp1: Asn^{321} and Asn^{335}; Nramp2: Asn^{336} and Asn^{349}) are indicated.

suggesting a significant difference in the extent of core and complex glycosylation in this chimeric protein (Fig. 2*A*). We examined the glycosylation status of N1N-HA using the glycosylation inhibitor tunicamycin. Incubation with tunicamycin resulted in a reduction in the amount of complex glycosylated species concomitant with an increase in the precursor unglycosylated species (supplemental Fig. 1). The N1N-HA precursor showed an apparent faster electrophoretic mobility that the precursor for Nramp2-HA, suggesting possible differences in post-translational modification of the two proteins in LLC-PK_1 cells unrelated to glycosylation. Nramp1 has been shown previously to be hyperphosphorylated (40), and differences in this or other types of modifications may account for the differences in mobility. N1C-HA was detected as two immunoreactive species of electrophoretic mobility similar to that of WT Nramp2. However, the proportion of the immature precursor N1C-HA protein (~60 kDa) appeared to be significantly greater than that found for WT Nramp2, suggesting possible incomplete maturation of this chimera (Fig. 2*A*). WT Nramp1 and chimeras N2N and N2C were detected as immunoreactive species of ~70–75 kDa (Fig. 2*A*, *bottom panel*). LLC-PK_1 cells expressing the different WT and chimeric proteins were treated with the translation inhibitor cycloheximide for different periods of time, and the fate of core glycosylated and mature protein isoforms was analyzed by immunoblotting (Fig. 2*B*). These experiments showed that WT Nramp2 and Nramp1 as well as the chimeras N1N-HA, N2N, and N2C quickly matured from a core glycosylated precursor to a fully mature form that remained stable for a 7-h period. Interestingly the N1C-HA chimera displayed increased persistence of precursor and

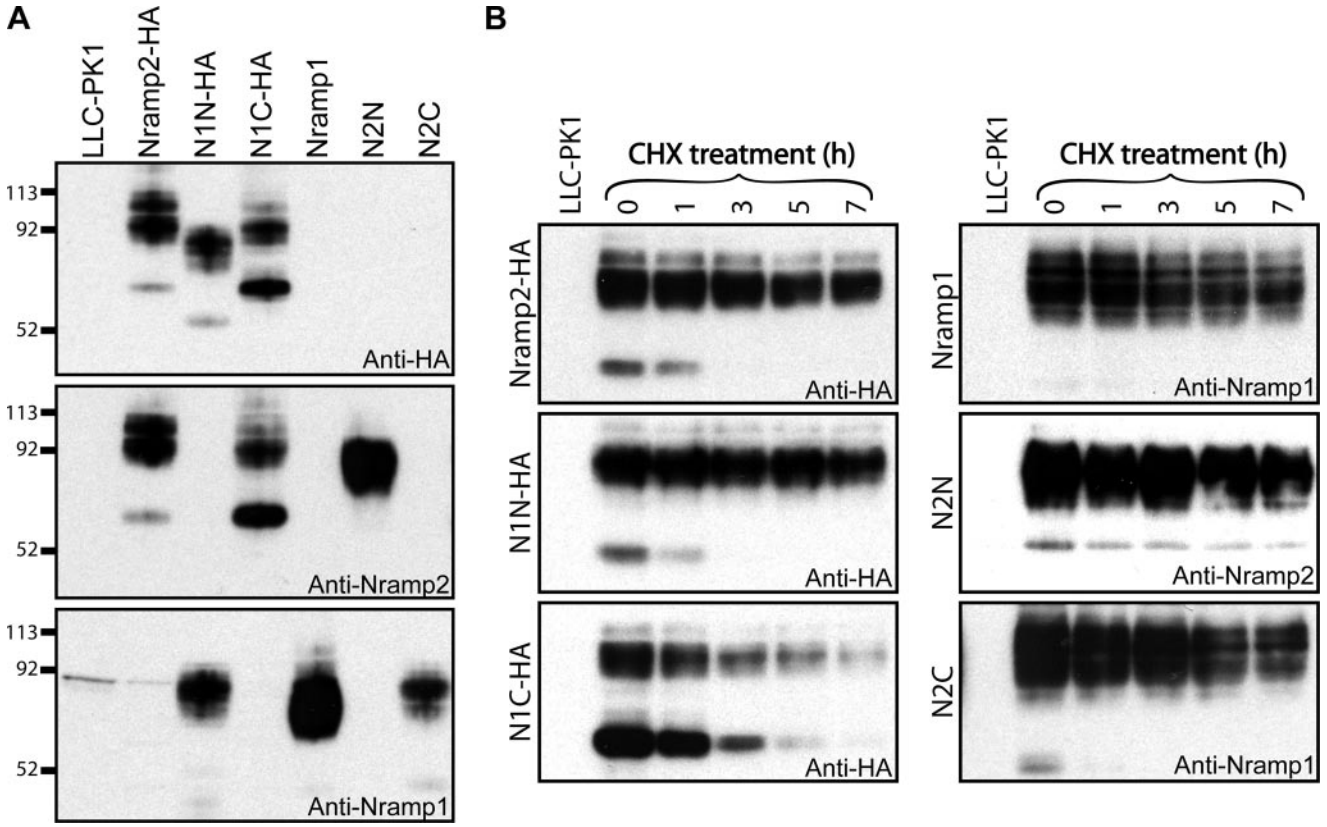

FIGURE 2. **Expression and stability of Nramp1/2 chimeras in transfected LLC-PK$_1$ cells.** Total cell extracts from untransfected cells (LLC-PK$_1$) and cell clones stably expressing wild-type Nramp1 (*Nramp1*), wild-type Nramp2 (*Nramp2-HA*), and the Nramp1/2 chimeras (*N1N-HA*, *N1C-HA*, *N2N*, and *N2C*) were resolved by SDS-PAGE and analyzed by immunoblotting. *A*, immunoblots were incubated with antibodies recognizing either the HA epitope (*anti-HA*), the amino terminus of Nramp2 (*anti-Nramp2*), or the amino terminus of Nramp1 (*anti-Nramp1*). The sizes of molecular mass standards (in kilodaltons) are indicated. In *B*, transfectants expressing the indicated proteins were treated with the translation inhibitor cycloheximide (*CHX*; 20 μg/ml) for 0, 1, 3, 5, or 7 h. Immunoblotting of total cell lysates was carried out to assess the stability of wild-type and chimeric proteins. Antibodies used for each blot are indicated.

reduced stability of the mature form compared with controls with little protein detectable at 7 h (Fig. 2*B*). These results suggest impaired processing of the N1C-HA chimera.

Cell Surface Expression of Chimeric Proteins—We used a cell surface biotinylation technique to quantify plasma membrane expression of the Nramp1/2 chimeras at steady state (27, 32). LLC-PK$_1$ cells stably expressing either WT or chimeric Nramp constructs were treated with a membrane-impermeable biotin compound to label all cell surface proteins. After solubilization, cell surface proteins were isolated with immobilized streptavidin followed by separation by SDS-PAGE and visualization by immunoblotting (Fig. 3*A*, *Surface*). Cell surface expression of each protein was then compared with total protein expression for each cell line (Fig. 3*A*, *Total*). WT Nramp2-HA and N1C-HA were detected at robust levels at the plasma membrane, whereas WT Nramp1, N1N-HA, N2N, and N2C displayed little or no cell surface expression (Fig. 3*A*). Clearly replacing either the amino (N2N) or carboxyl (N2C) termini of Nramp1 with the equivalent segments of Nramp2 did not result in plasma membrane expression. Because Nramp2-HA, N1N-HA, and N1C-HA were constructed with exofacial HA tags in predicted EC4, the fraction of each variant present at the cell surface at steady state could be determined by exposing fixed LLC-PK$_1$ transfectants to anti-HA antibody with (total expression) or without (cell surface) prior permeabilization with detergent. The amount of bound anti-HA antibody was quantified using a secondary antibody coupled to horseradish peroxidase. We determined that 35.9 $\pm$ 3.9% (mean $\pm$ S.E.) of WT Nramp2-HA and 21.3 $\pm$ 1.3% of N1C-HA were expressed at the cell surface compared with a modest 0.5 $\pm$ 1.2% for N1N-HA (Fig. 3*B*). These values are consistent with cell surface biotinylation results (Fig. 3*A*) and suggest that the amino terminus of Nramp1 impairs normal targeting of Nramp2 to the plasma membrane.

Nramp2 isoform II is normally expressed at the plasma membrane and in recycling endosomes in LLC-PK$_1$ cells. Replacing the carboxyl terminus of Nramp2-HA with the equivalent segment of Nramp1 (N1C-HA) did not have a major effect on the cell surface expression of the transporter (Fig. 3, *A* and *B*). Interestingly despite the impaired processing and reduced stability, N1C-HA retained significant metal transport activity (Fig. 3*C*). This activity likely stems from the significant fraction of mature N1C-HA protein that is expressed at the cell surface. On the other hand, replacing the amino terminus of Nramp2-HA with the equivalent segment from Nramp1 (N1N-HA) drastically reduced surface expression (Fig. 3, *A* and *B*) as well as metal transport activity (Fig. 3*C*). This result suggests that the amino terminus of Nramp1 contains targeting information that affects the normal trafficking of Nramp2 to the plasma membrane.

Subcellular Localization of Chimeric Proteins—Immunofluorescence was used to compare the subcellular localization of wild-type and chimeric proteins at steady state. LLC-PK$_1$ trans-

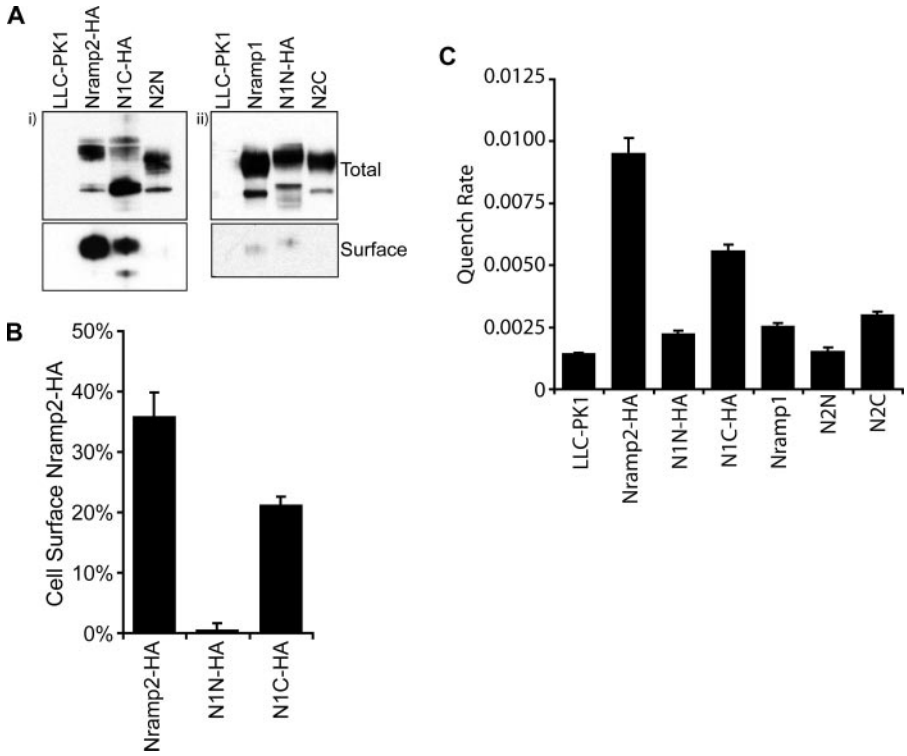

FIGURE 3. **Cell surface expression and metal transport activity of the Nramp1/2 chimeras.** *A*, cell surface biotinylation was used to assess plasma membrane expression of wild-type Nramp1 (*Nramp1*), wild-type Nramp2 (*Nramp2-HA*), and the Nramp1/2 chimeras (*N1N-HA*, *N1C-HA*, *N2N*, and *N2C*). Live cells were labeled with a membrane-impermeable biotin compound (see "Experimental Procedures"). Total cell protein extracts were prepared, and biotinylated proteins were isolated by affinity capture with streptavidin-agarose beads. Equivalent amounts of total cell extracts (*Total*) and captured biotinylated protein (*Surface*) were resolved by SDS-PAGE followed by immunoblotting with anti-Nramp2 (*i*) or anti-Nramp1 (*ii*) polyclonal antibodies. *B*, the fraction of Nramp2-HA, N1N-HA, and N1C-HA expressed at the cell surface was quantified using the exofacial HA epitope tag inserted in predicted extracytoplasmic loop 4 of those proteins. Briefly cells were fixed and incubated with primary anti-HA antibody with or without prior detergent permeabilization followed by incubation with a horseradish peroxidase-coupled secondary antibody and quantification by a colorimetric assay. The amount of Nramp proteins expressed at the cell surface (in non-permeabilized cells) is shown as a fraction (%) of total protein expression (in permeabilized cells). In *C*, metal transport activity of the Nramp1/2 chimeras was determined using a fluorescence quenching assay. Cells loaded with a metal-sensitive fluorescent dye were incubated with Co^{2+} in acidic buffer. Results are shown as the initial rates of fluorescence quenching. *Error bars* represent S.E. of three or more independent determinations.

fectants were fixed and permeabilized, and chimeric proteins were labeled with polyclonal antibodies recognizing either Nramp1 or Nramp2. Consistent with our previously published data (32, 36), Nramp2-HA displayed strong colocalization with GFP-syntaxin 13, whereas Nramp1 showed little overlap with the recycling endosome marker (Fig. 4*A*). Interestingly all chimeras showed no significant colocalization with GFP-syntaxin 13 (Fig. 4*A*). These results suggest that substitution of either the amino or carboxyl terminus of Nramp2 by homologous segments of Nramp1 impairs targeting to the recycling endosome compartment.

Consistent with previously published data (8), Nramp1 showed strong colocalization with the lysosomal marker GFP-Lamp1, whereas Nramp2-HA displayed little colocalization with this marker (Fig. 4*B*). These results confirm that Nramp1 is properly targeted to the lysosomal compartment in LLC-PK_1 cells. Remarkably all chimeras displayed significant colocalization with GFP-Lamp1 (Fig. 4*B*), indicating their presence in late endosomes and lysosomes. Clearly replacing the amino or carboxyl termini of Nramp1 with the equivalent regions of Nramp2 (N2N and N2C) did not significantly affect the subcellular distribution of Nramp1 at steady state (Table 1). Previous work by us and others has demonstrated that the carboxyl terminus of Nramp2 isoform II contains targeting information (including a YLLNT signal) crucial for endocytosis and recycling of the transporter from the plasma membrane (31, 32). Mutations or deletions in this motif result in a protein that has impaired recycling following internalization from the cell surface and accumulates in the lysosomal compartment (32). Consistent with these findings, replacing the carboxyl terminus of Nramp2 with the equivalent segment from Nramp1 (N1C-HA) resulted in plasma membrane expression (Fig. 3) and lysosomal targeting (Fig. 4*B* and Table 1). Therefore, the mistargeting displayed by N1C-HA is probably due to removal of the carboxyl terminus of Nramp2 rather than the presence of a dominant targeting signal in the carboxyl terminus of Nramp1. A fraction of N1C-HA showed some colocalization with the endoplasmic reticulum marker GFP-Sec61 (data not shown), suggesting that some N1C-HA may be retained in the ER. Finally substituting the amino terminus of Nramp2 with the equivalent segment from Nramp1 (N1N-HA) yielded the most intriguing result. N1N-HA showed subcellular localization indistinguishable from WT Nramp1 with no significant surface expression (Table 1) but strong lysosomal targeting (Fig. 4*B*). These results suggest that the amino terminus of Nramp1 possesses lysosomal targeting information that can act in a dominant fashion over the recycling endosome signal present in the carboxyl terminus of Nramp2 isoform II.

Characterization of the YSGI Motif in the Amino Terminus of Nramp1—Closer examination of the predicted cytoplasmic amino-terminal region of Nramp1 revealed a ^{15}YGSI^{18} motif that fits the Y*XX*Φ consensus signature (Fig. 1*A*). Y*XX*Φ motifs have been implicated in targeting membrane proteins such as LAMP-1 and LAMP-2 to lysosomes by interacting with the μ subunits of AP-1 and AP-2 complexes (33, 41–44). To determine whether the YGSI motif in the amino terminus of Nramp1 was responsible for the lysosomal targeting of the N1N-HA chimera, we created alanine substitutions at each position of the YGSI signal within the N1N-HA chimeric construct. The mutants were stably transfected into LLC-PK_1 cells, and clones positive for expression were selected for analysis. Immunoblot analysis performed on cell extracts showed stable expression of Y15A, G16A, and S17A mutants at levels comparable to N1N-

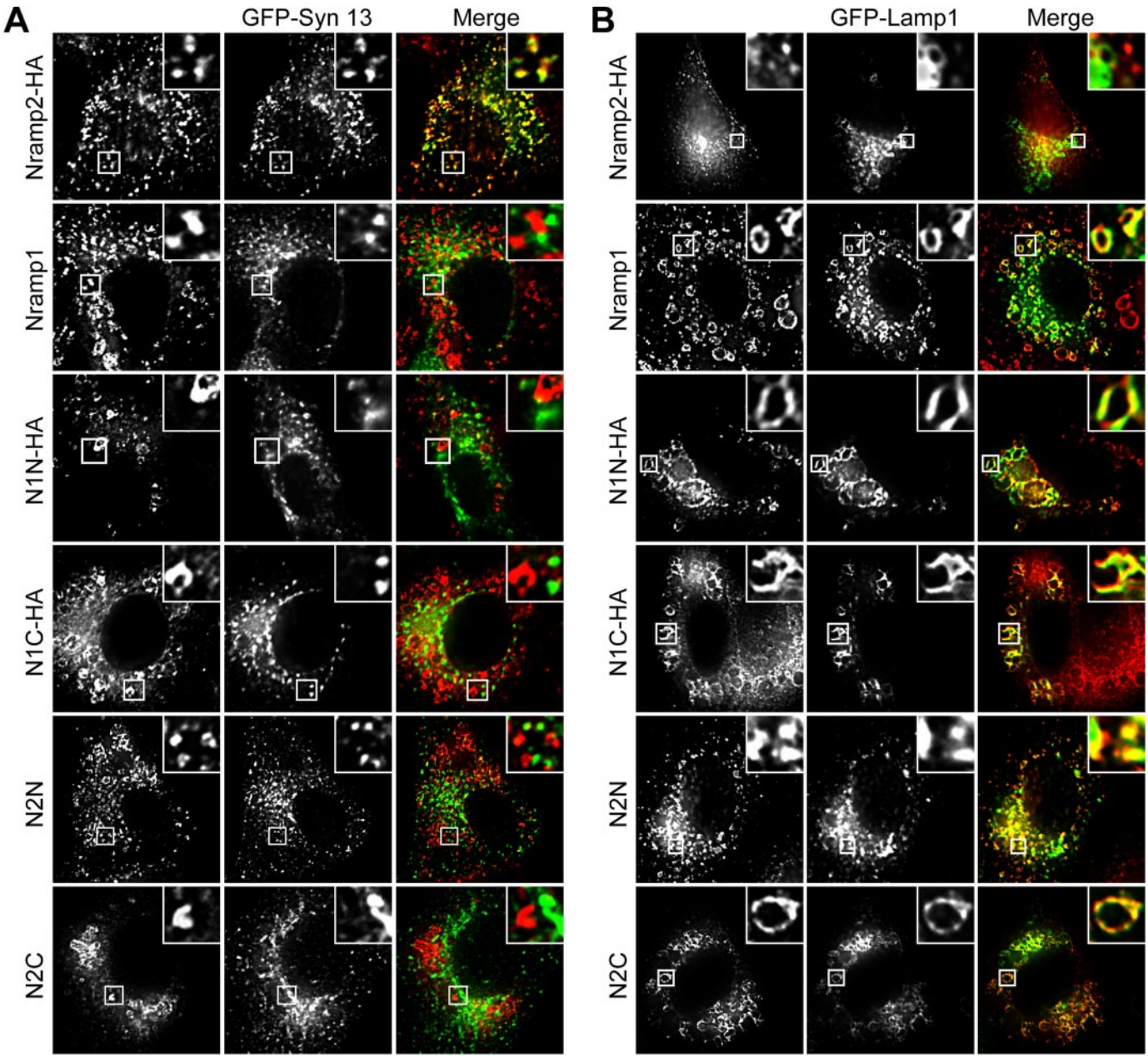

FIGURE 4. **Subcellular localization of Nramp1/2 chimeras.** LLC-PK$_1$ cells stably expressing wild-type Nramp1 (*Nramp1*), wild-type Nramp2 (*Nramp2-HA*), and the Nramp1/2 chimeras (*N1N-HA*, *N1C-HA*, *N2N*, and *N2C*) were transiently transfected with either GFP-syntaxin 13 to label recycling endosomes (*A*) or GFP-Lamp1 to label late endosomes and lysosomes (*B*). Twenty-four hours later, cells were fixed, permeabilized, and stained with either anti-Nramp1 or anti-Nramp2 polyclonal antibodies followed by a secondary antibody coupled to fluorescent Cy3. Images were acquired by epifluorescence microscopy. *Insets* show magnifications of the area *boxed* in the figure.

TABLE 1
Subcellular localization of Nramp1/2 chimeras

	Plasma membrane	Recycling endosomes	Late endosomes and lysosomes	Endoplasmic reticulum
Nramp2-HA	+	+	−	−
N1N-HA	−	−	+	−
N1C-HA	+	−	+	+
Nramp1	−	−	+	−
N2N	−	−	+	−
N2C	−	−	+	−

HA, although lower expression was detected for I18A (Fig. 5*A*). We determined the fraction of each N1N-HA expressed at the cell surface. Mutating any of the residues in the YGSI motif to alanine increased the surface expression of the chimera (Fig. 5*B*). Y15A demonstrated the highest surface expression (19.2 ± 2.0%) followed by S17A (10.2 ± 1.2%), I18A (7.4 ± 2.1%), and G16A (4.4 ± 0.3%). This increase in surface expression was concomitant to a commensurate increase in metal transport activity for the mutants (Fig. 5*C*), implying that N1N-HA is indeed properly folded in a transport-competent manner at the cell surface.

We determined the subcellular localization of the N1N-HA mutants at steady state in fixed and permeabilized cells. Mutants G16A and S17A displayed subcellular localization similar to N1N-HA, showing little colocalization with the recy-

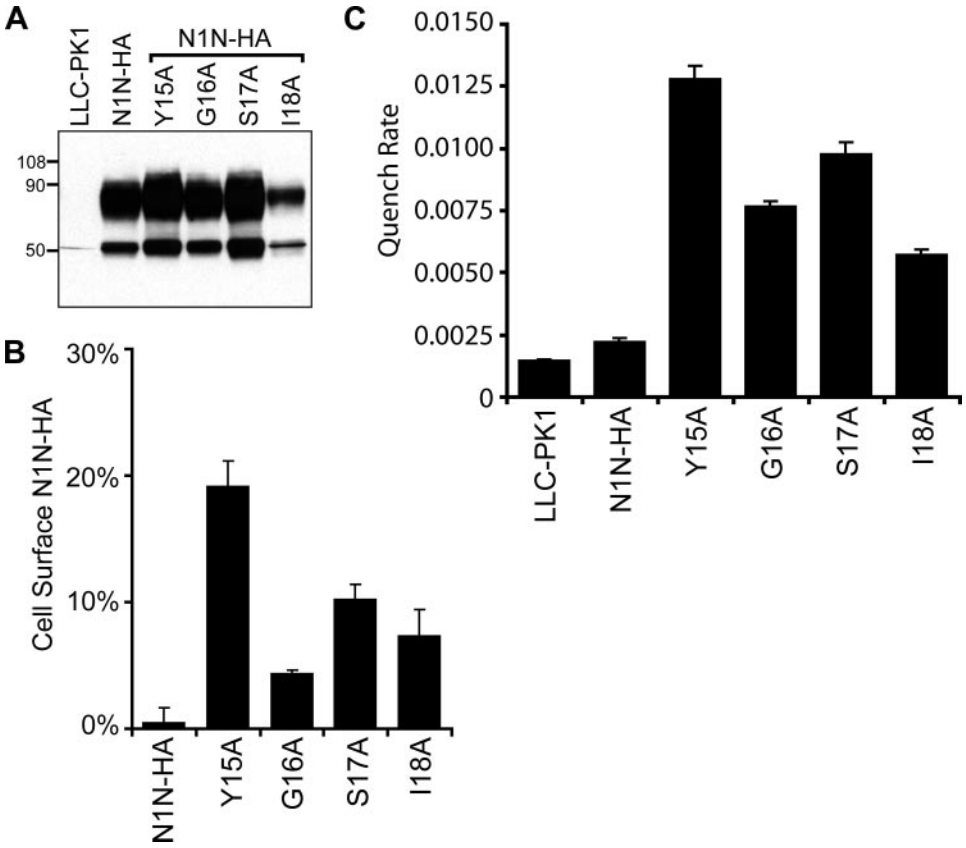

FIGURE 5. **Characterization of N1N-HA targeting motif mutants.** *A*, total cell extracts were prepared from transfectants stably expressing individual mutants (Y15A, G16A, S17A, and I18A) in the putative YGSI lysosomal targeting motif present in the N1N-HA backbone. Equal amounts of cell extract were resolved by SDS-PAGE and analyzed by immunoblotting with anti-HA antibody. The sizes of molecular mass standards (in kilodaltons) are indicated. In *B*, the fraction of N1N-HA expressed at the cell surface was determined as described in the legend of Fig. 3*B*. *C*, metal transport activity of the N1N-HA targeting motif mutants was measured by quenching of calcein fluorescence as described in the legend of Fig. 3*C*. *Error bars* represent S.E. of three or more independent determinations.

cling endosome marker GFP-syntaxin 13 (Fig. 6*A*) but strong colocalization with the lysosomal marker GFP-Lamp1 (Fig. 6*B*). These results suggest that Gly[16] and Ser[17] are not essential for the lysosomal targeting of N1N-HA. Strikingly mutants Y15A and I18A displayed subcellular localization similar to WT Nramp2, showing strong colocalization with syntaxin 13-positive recycling endosomes (Fig. 6*A*) but little colocalization with Lamp1-positive lysosomes (Fig. 6*B* and summarized in Table 2). These results suggest that Tyr[15] and Ile[18] are critical for the lysosomal targeting of N1N-HA and that the YGSI motif in the amino terminus of Nramp1 functions as a *YXX*Φ lysosomal targeting signal. Furthermore this YGSI signal appears to dominate the recycling endosome signal present in the carboxyl terminus of Nramp2 isoform II.

DISCUSSION

In this study, we sought to investigate the subcellular targeting and trafficking properties of Nramp1, including the identification of sorting signals responsible for its distinct localization in lysosomes of mononuclear phagocytes. For this, we constructed chimeric proteins in which homologous domains of Nramp1 and the closely related iron transporter Nramp2 (isoform II) were exchanged. Replacing the amino (N2N) or carboxyl (N2C) terminal cytoplasmic segments of Nramp1 with the equivalent segments from Nramp2 did not drastically affect the expression or subcellular localization of the transporter. Indeed both N2N and N2C chimeras exhibited little cell surface expression but showed strong lysosomal targeting typical of WT Nramp1. These results suggested that sorting signals in the amino and carboxyl cytoplasmic termini of Nramp2 are unable to confer cell surface and/or recycling endosome targeting to the Nramp1 backbone. Results with the N2N chimera are supported by our previous work showing that deletion mutations at putative sorting signals in the amino terminus of Nramp2 do not significantly affect the cell surface or recycling endosome targeting of the transporter (32). In contrast, we and other groups have shown that a YLLNT motif in the carboxyl terminus of Nramp2 isoform II controls the internalization and recycling of the protein from plasma membrane (31, 32). However, results with the N2C chimera suggested that this YLLNT motif was somehow masked or non-functional when placed on the background of Nramp1.

An Nramp2-HA chimera bearing the carboxyl-terminal cytoplasmic segment of Nramp1 (N1C-HA) was robustly expressed in LLC-PK$_1$ cells but displayed a higher fraction of a ~60-kDa precursor species and a lower fraction of the ~90-kDa mature protein, suggesting impaired processing of this chimera. N1C-HA also displayed reduced stability. Surface biotinylation experiments revealed that the mature, fully glycosylated N1C-HA was expressed at the cell surface (Fig. 2*A*) and was likely responsible for the residual metal transport activity observed for this construct (Fig. 2*C*). This result suggests that complex glycosylation acquired by the precursor protein in the Golgi apparatus is critical for the plasma membrane targeting of mature Nramp2. However, a more likely explanation is that processing of the oligosaccharides is merely a reflection that the proteins were folded well enough to exit the ER and thereafter acquire complex glycosylation. Strikingly the multiple biosynthetic and functional defects of the N1C-HA chimera virtually mirror those observed for the Nramp2^{G185R} mutant protein produced in *mk* mice and Belgrade rats (37). Although a small fraction of N1C-HA displayed some colocalization with the ER marker GFP-Sec61 (data not shown), a more significant fraction of the chimera was expressed in late endosomes and lysosomes. We have shown previously that critical mutations at the carboxyl terminus of Nramp2 isoform II (including a truncation of the entire carboxyl-terminal segment) result in a protein that is unable to recycle

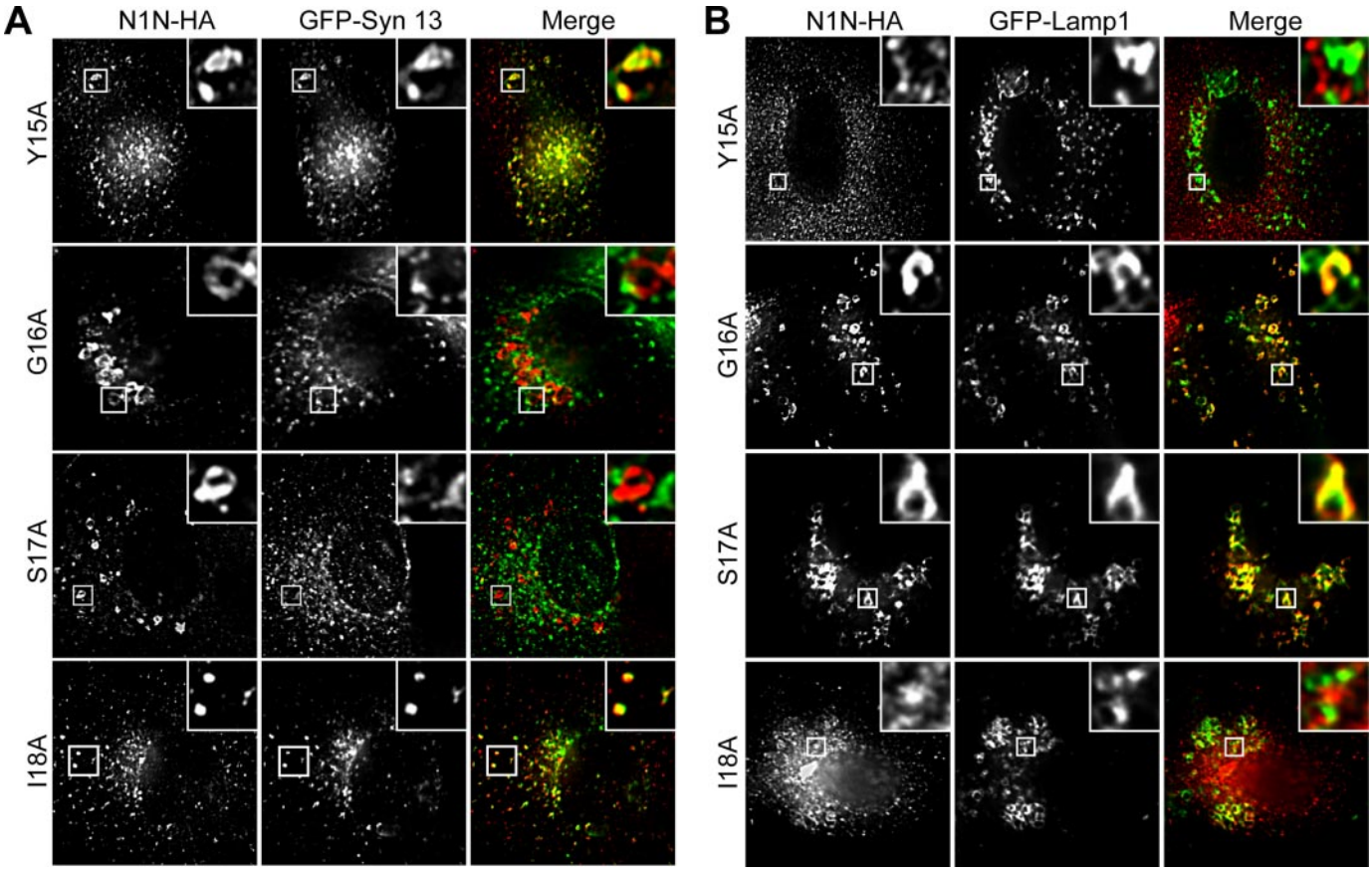

FIGURE 6. **Subcellular localization of N1N-HA mutants.** LLC-PK$_1$ cells stably expressing N1N-HA YGSI mutants were transiently transfected with either the recycling endosome marker GFP-syntaxin 13 (*A*) or the late endosomal and lysosomal marker GFP-Lamp1 (*B*). Twenty-four hours later, cells were fixed, permeabilized, and stained with an anti-Nramp1 polyclonal antibody followed by a secondary antibody coupled to fluorescent Cy3. Images were acquired by epifluorescence microscopy. *Insets* show magnifications of the area *boxed* in the figure.

TABLE 2
Subcellular localization of N1N-HA mutants

	Plasma membrane	Recycling endosomes	Late endosomes and lysosomes	Endoplasmic reticulum
N1N-HA	−	−	+	−
Y15A	+	+	−	−
G16A	+	−	+	−
S17A	+	−	+	−
I18A	+	+	−	−

after internalization from the cell surface and is targeted to the lysosomes by default (32). Therefore, we reasoned that the lysosomal targeting displayed by N1C-HA likely results from the removal of the carboxyl terminus of Nramp2 rather than the presence of a dominant targeting signal in the carboxyl terminus of Nramp1.

An Nramp2 chimera bearing the amino terminus of Nramp1 (N1N-HA) yielded perhaps the most intriguing results. N1N-HA was stably expressed in transfected LLC-PK$_1$ cells as a protein of lower apparent molecular weight compared with Nramp2-HA (Fig. 2*A*) probably due to altered glycosylation of the chimera. Interestingly the extent of glycosylation of N1N-HA resembled more closely that of Nramp1 (Fig. 2*A*) and raises the possibility that the amino terminus of Nramp2 contains sequence information that affects the extent of glycosylation of the transporter either directly or indirectly by mediating its trafficking and retention to specific subcellular compartments. Strikingly N1N-HA also displayed subcellular targeting properties similar to Nramp1 with no surface expression yet strong lysosomal targeting (Figs. 3 and 4). These results strongly suggested that the amino-terminal cytoplasmic segment of Nramp1 contained lysosomal targeting information that was able to act in a dominant fashion over a known recycling endosome targeting signal (^{555}YLLNT^{559}) in the carboxyl terminus of Nramp2 isoform II present in N1N-HA. The lack of significant transport activity for N1N-HA, as for Nramp1, likely resulted from the lack of expression at the site of transport measurements (plasma membrane) rather than expression of a non-functional protein (Fig. 3). Closer examination of the amino acid sequence within the amino terminus of Nramp1 revealed a potential tyrosine-based signal of the form *YXX*Φ (^{15}YGSI^{18}) (Fig. 1*A*). Alanine substitution mutations at Tyr^{15} and Ile^{18} within the N1N-HA chimera were able to restore cell surface and recycling endosome targeting of the Nramp2 chimera (Figs. 5*B* and 6*B*). However, alanine mutations at Gly^{16} and Ser^{17} of N1N-HA retained their lysosomal targeting (Fig. 6*B*). These results clearly demonstrate that ^{15}YGSI^{18} functions as a lysosomal targeting motif that fits the consensus *YXX*Φ in the amino terminus of Nramp1. *YXX*Φ signals have been shown to function as lysosomal sorting motifs in membrane proteins such as LAMP-1 (YQTI) (45). *YXX*Φ signals are known to bind the μ subunits of AP complexes strictly through their Y and Φ residues; however, the *X* residues and other residues flanking the motif contribute to the strength and specificity of the sig-

nals (33). Although the ^{15}YGSI^{18} motif in the amino terminus of Nramp1 can clearly function as a lysosomal targeting signal, other determinants within Nramp1 also appear to be important for lysosomal targeting of the protein. This is supported by two observations. First, the N2N chimera, which bears the amino terminus of Nramp2 on the backbone of Nramp1, was able to retain its lysosomal targeting despite lacking the YGSI motif. However, we cannot exclude the possibility that the ^{62}YSCF^{65} motif present in the amino terminus of Nramp2 may function as a lysosomal targeting signal in N2N that is normally masked by the presence of the recycling endosome targeting motif in the carboxyl terminus of Nramp2 isoform II (^{555}YLLNT^{559}). Second, YGSI signal mutants introduced into WT Nramp1 seemed to retain their lysosomal localization (supplemental Fig. 3, A and B). However, we noted that some of the Nramp1 YGSI mutants displayed an increased amount of plasma membrane expression measured by cell surface biotinylation that is not normally seen for WT Nramp1 (supplementary Fig. 2A). This increase in cell surface expression was concomitant with an increase in metal transport activity at the plasma membrane (supplemental Fig. 2B). The increased cell surface expression of certain Nramp1 YGSI mutants suggests that the plasma membrane may be a default pathway for Nramp1 that may be positively modulated by the YGSI motif to direct lysosomal targeting.

The identification of an Nramp1 lysosomal targeting signal allows us to propose a model for the role of cytoplasmic motifs in subcellular trafficking of Nramp1 and Nramp2. In this model (Fig. 7), Nramp2 isoform II is synthesized in the ER, targeted to the Golgi apparatus for complex glycosylation, and dispatched to the plasma membrane. At the cell surface, Nramp2 recruits specific adaptor proteins required for rapid clathrin-mediated endocytosis through binding to a YLLNT motif present in its carboxyl terminus. Nramp2 is then internalized into early endosomes, and the recruited adaptor complexes are involved in signaling the recycling of the transporter back to the cell surface via recycling endosomes (Fig. 7). This pathway is shared by the transferrin receptor and is of critical importance for iron acquisition from transferrin following acidification of the endosomes and Nramp2-mediated translocation of iron to the cytoplasm. Similar to Nramp2, Nramp1 is targeted from the ER to the Golgi for complex glycosylation. However, the recognition of the YGSI signal by specific adaptor proteins mediates the sorting of Nramp1 directly from the trans-Golgi network to late endosomes and lysosomes (Fig. 7). The N1N-HA chimera, which possesses the Nramp1 YGSI signal, is targeted in a fashion similar to WT Nramp1 with the amino-terminal lysosomal signal taking precedence over the carboxyl-terminal YLLNT recycling signal. N1N-HA^{Y15A} and N1N-HA^{I18A} mutants are unable to recruit lysosomal sorting proteins and are targeted to recycling endosomes via the carboxyl-terminal YLLNT signal in a fashion similar to WT Nramp2 (Fig. 7). On the other hand, although alanine mutations at Gly^{16} and Ser^{17} of N1N-HA do not drastically affect lysosomal targeting; the mutations may reduce the effectiveness of the Y*XX*Φ signal. This reduced sorting efficiency may result in a higher fraction of N1N-HA^{G16A} and

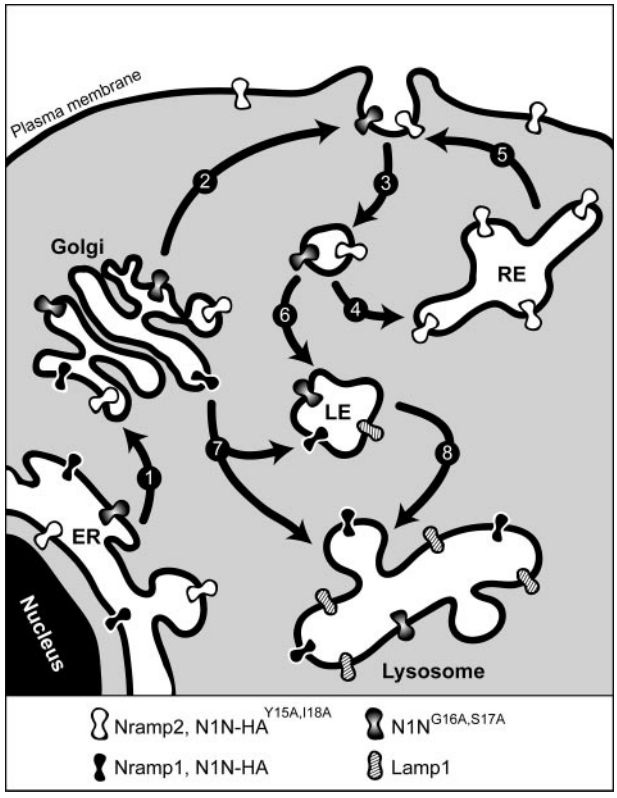

FIGURE 7. **Model for subcellular trafficking of Nramp1 and Nramp2 (isoform II).** Nramp2 isoform II is synthesized in the ER, targeted to the Golgi apparatus (*step 1*) for complex glycosylation, and targeted to the plasma membrane (*step 2*). At the cell surface, Nramp2 is internalized via a clathrin- and dynamin-dependent process by recruiting adaptor proteins that specifically recognize the carboxyl-terminal YLLNT motif (*step 3*). Nramp2 is then targeted to early endosomes, and the interaction of YLLNT with adaptor proteins mediates its recycling back to the cell surface via recycling endosomes (*steps 4* and *5*). Nramp1 is similarly trafficked to the Golgi after synthesis (*step 1*). However, recognition of the YGSI signal by lysosomal sorting proteins mediates its targeting from the trans-Golgi network directly to late endosomes and lysosomes (*steps 7* and *8*). The Nramp2-HA chimera N1N-HA, which possesses the Nramp1 amino-terminal YGSI signal, is targeted in a fashion similar to WT Nramp1. N1N-HA^{Y15A} and N1N-HA^{I18A} mutants are unable to recruit lysosomal sorting proteins and are targeted to recycling endosomes via the carboxyl-terminal YLLNT signal in a fashion similar to WT Nramp2. N1N-HA^{G16A} and N1N-HA^{S17A} mutants are sorted less efficiently to lysosomes, leading to some cell surface accumulation. These mutants, however, are not recycled upon internalization and are ultimately targeted to lysosomes via the normal endocytic pathway. *RE*, recycling endosomes; *LE*, late endosomes.

N1N-HA^{S17A} mutants being sorted to the cell surface and subsequently targeted to the lysosomal compartment via the endocytic pathway (Fig. 7). It has been shown that mutations in the *X* residues or in other residues neighboring the Y*XX*Φ signal can impair lysosomal targeting without significantly disrupting internalization (43, 46, 47). An indirect targeting of N1N-HA^{G16A} and N1N-HA^{S17A} mutants to lysosomes via the plasma membrane would explain the increased cell surface expression observed for these mutants (Fig. 5*B*). Another possibility is that WT Nramp1 normally traffics to the lysosome via rapid internalization from the plasma membrane. However, a large amount of published data indicates that there is little if any Nramp1 expression at the cell surface at steady state (8, 13, 34), suggesting that any trafficking through the plasma membrane must be a minor component of the overall lysosomal targeting pathway for Nramp1.

Interestingly the YGSI signal in Nramp1 does not completely conform to the Y*XX*Φ signals found in several other lysosomal proteins, raising the possibility that YGSI may represent a novel subset of Y*XX*Φ signals. Two common features of Y*XX*Φ signals involved in lysosomal targeting seem to be the presence of a glycine residue preceding the critical tyrosine as well as the prevalence of the motifs in the carboxyl terminus of membrane proteins (33). Nramp1 possesses a serine instead of a glycine upstream of its YGSI signal. Also the YGSI signal is found in the amino terminus of the protein as opposed to the more commonly found carboxyl terminus. Amino-terminal Y*XX*Φ motifs have been identified in proteins such as the transferrin receptor (YTRF) but function typically as endocytic signals. Additional experiments are needed to identify the specific binding partners of YGSI and better understand the molecular machinery involved in the sorting of Nramp1 to late endosomes and lysosomes. Hopefully the characterization of other tyrosine-based signals in the cytoplasmic domains of lysosomal proteins will clarify whether the YGSI motif in Nramp1 represents a novel subset of Y*XX*Φ motifs.

Clearly proper lysosomal targeting of Nramp1 is critical for its antimicrobial activity as a metal efflux pump at the phagosomal membrane of macrophages and other phagocytic cells. Upon phagocytosis of a live pathogen, Nramp1-positive lysosomes fuse with the membranes of the pathogen-containing phagosomes, and Nramp1 remains associated with the phagosomes through their maturation to fully antimicrobial phagolysosomes (8). Our discovery that a sequence motif in the amino terminus of Nramp1 is sufficient to target Nramp proteins to the lysosomes suggests a model for functional evolution of Nramp proteins. In this model, Nramp1 and Nramp2 were generated by gene duplication from a common ancestor followed by subsequent sequence divergence to retain function with respect to mechanism of transport and ion selectivity. Further divergence, including (*a*) restriction of *Nramp1* transcriptional activity to cells of the mononuclear and polymorphonuclear phagocyte lineages and (*b*) acquisition of a targeting signal in the amino terminus (YGSI) actively directing Nramp1 localization to lysosomes for delivery to pathogen-containing phagosomes, would have ensued to enable metal efflux at the phagosomal membrane. This activity appears to have been extremely beneficial to the host and has been preserved throughout evolution from lower eukaryotes to humans (17).

REFERENCES

1. Forbes, J. R., and Gros, P. (2001) *Trends Microbiol.* **9,** 397–403
2. Vidal, S. M., Malo, D., Vogan, K., Skamene, E., and Gros, P. (1993) *Cell* **73,** 469–485
3. Malo, D., Vogan, K., Vidal, S., Hu, J., Cellier, M., Schurr, E., Fuks, A., Bumstead, N., Morgan, K., and Gros, P. (1994) *Genomics* **23,** 51–61
4. Vidal, S., Gros, P., and Skamene, E. (1995) *J. Leukoc. Biol.* **58,** 382–390
5. Abel, L., Sanchez, F. O., Oberti, J., Thuc, N. V., Hoa, L. V., Lap, V. D., Skamene, E., Lagrange, P. H., and Schurr, E. (1998) *J. Infect. Dis.* **177,** 133–145
6. Bellamy, R., Ruwende, C., Corrah, T., McAdam, K. P., Whittle, H. C., and Hill, A. V. (1998) *N. Engl. J. Med.* **338,** 640–644
7. Awomoyi, A. A., Marchant, A., Howson, J. M., McAdam, K. P., Blackwell, J. M., and Newport, M. J. (2002) *J. Infect. Dis.* **186,** 1808–1814
8. Gruenheid, S., Pinner, E., Desjardins, M., and Gros, P. (1997) *J. Exp. Med.* **185,** 717–730
9. Searle, S., Bright, N. A., Roach, T. I., Atkinson, P. G., Barton, C. H., Meloen, R. H., and Blackwell, J. M. (1998) *J. Cell Sci.* **111,** 2855–2866
10. Govoni, G., Canonne-Hergaux, F., Pfeifer, C. G., Marcus, S. L., Mills, S. D., Hackam, D. J., Grinstein, S., Malo, D., Finlay, B. B., and Gros, P. (1999) *Infect. Immun.* **67,** 2225–2232
11. Cuellar-Mata, P., Jabado, N., Liu, J., Furuya, W., Finlay, B. B., Gros, P., and Grinstein, S. (2002) *J. Biol. Chem.* **277,** 2258–2265
12. Jabado, N., Jankowski, A., Dougaparsad, S., Picard, V., Grinstein, S., and Gros, P. (2000) *J. Exp. Med.* **192,** 1237–1248
13. Forbes, J. R., and Gros, P. (2003) *Blood* **102,** 1884–1892
14. Jabado, N., Cuellar-Mata, P., Grinstein, S., and Gros, P. (2003) *Proc. Natl. Acad. Sci. U. S. A.* **100,** 6127–6132
15. Gruenheid, S., Cellier, M., Vidal, S., and Gros, P. (1995) *Genomics* **25,** 514–525
16. Gunshin, H., Mackenzie, B., Berger, U. V., Gunshin, Y., Romero, M. F., Boron, W. F., Nussberger, S., Gollan, J. L., and Hediger, M. A. (1997) *Nature* **388,** 482–488
17. Cellier, M., Prive, G., Belouchi, A., Kwan, T., Rodrigues, V., Chia, W., and Gros, P. (1995) *Proc. Natl. Acad. Sci. U. S. A.* **92,** 10089–10093
18. Canonne-Hergaux, F., Gruenheid, S., Ponka, P., and Gros, P. (1999) *Blood* **93,** 4406–4417
19. Canonne-Hergaux, F., Zhang, A. S., Ponka, P., and Gros, P. (2001) *Blood* **98,** 3823–3830
20. Hentze, M. W., Muckenthaler, M. U., and Andrews, N. C. (2004) *Cell* **117,** 285–297
21. Canonne-Hergaux, F., and Gros, P. (2002) *Kidney Int.* **62,** 147–156
22. Fleming, M. D., Trenor, C. C., III, Su, M. A., Foernzler, D., Beier, D. R., Dietrich, W. F., and Andrews, N. C. (1997) *Nat. Genet.* **16,** 383–386
23. Fleming, M. D., Romano, M. A., Su, M. A., Garrick, L. M., Garrick, M. D., and Andrews, N. C. (1998) *Proc. Natl. Acad. Sci. U. S. A.* **95,** 1148–1153
24. Gunshin, H., Fujiwara, Y., Custodio, A. O., Direnzo, C., Robine, S., and Andrews, N. C. (2005) *J. Clin. Investig.* **115,** 1258–1266
25. Mims, M. P., Guan, Y., Pospisilova, D., Priwitzerova, M., Indrak, K., Ponka, P., Divoky, V., and Prchal, J. T. (2005) *Blood* **105,** 1337–1342
26. Iolascon, A., d'Apolito, M., Servedio, V., Cimmino, F., Piga, A., and Camaschella, C. (2006) *Blood* **107,** 349–354
27. Lam-Yuk-Tseung, S., Mathieu, M., and Gros, P. (2005) *Blood Cells Mol. Dis.* **35,** 212–216
28. Priwitzerova, M., Nie, G., Sheftel, A. D., Pospisilova, D., Divoky, V., and Ponka, P. (2005) *Blood* **106,** 3985–3987
29. Gunshin, H., Jin, J., Fujiwara, Y., Andrews, N. C., Mims, M., and Prchal, J. (2005) *Blood* **106,** 2221–2222
30. Gruenheid, S., Canonne-Hergaux, F., Gauthier, S., Hackam, D. J., Grinstein, S., and Gros, P. (1999) *J. Exp. Med.* **189,** 831–841
31. Tabuchi, M., Tanaka, N., Nishida-Kitayama, J., Ohno, H., and Kishi, F. (2002) *Mol. Biol. Cell* **13,** 4371–4387
32. Lam-Yuk-Tseung, S., Touret, N., Grinstein, S., and Gros, P. (2005) *Biochemistry* **44,** 12149–12159
33. Bonifacino, J. S., and Traub, L. M. (2003) *Annu. Rev. Biochem.* **72,** 395–447
34. Picard, V., Govoni, G., Jabado, N., and Gros, P. (2000) *J. Biol. Chem.* **275,** 35738–35745
35. Lam-Yuk-Tseung, S., Govoni, G., Forbes, J., and Gros, P. (2003) *Blood* **101,** 3699–3707
36. Touret, N., Furuya, W., Forbes, J., Gros, P., and Grinstein, S. (2003) *J. Biol. Chem.* **278,** 25548–25557
37. Touret, N., Martin-Orozco, N., Paroutis, P., Furuya, W., Lam-Yuk-Tseung, S., Forbes, J., Gros, P., and Grinstein, S. (2004) *Blood* **104,** 1526–1533
38. Lam-Yuk-Tseung, S., and Gros, P. (2006) *Biochemistry* **45,** 2294–2301
39. Lam-Yuk-Tseung, S., Camaschella, C., Iolascon, A., and Gros, P. (2006) *Blood Cells Mol. Dis.* **36,** 347–354
40. Vidal, S. M., Pinner, E., Lepage, P., Gauthier, S., and Gros, P. (1996) *J. Immunol.* **157,** 3559–3568
41. Ohno, H., Stewart, J., Fournier, M. C., Bosshart, H., Rhee, I., Miyatake, S., Saito, T., Gallusser, A., Kirchhausen, T., and Bonifacino, J. S. (1995) *Sci-*

ence **269,** 1872–1875
42. Boll, W., Ohno, H., Songyang, Z., Rapoport, I., Cantley, L. C., Bonifacino, J. S., and Kirchhausen, T. (1996) *EMBO J.* **15,** 5789–5795
43. Rohrer, J., Schweizer, A., Russell, D., and Kornfeld, S. (1996) *J. Cell Biol.* **132,** 565–576
44. Guarnieri, F. G., Arterburn, L. M., Penno, M. B., Cha, Y., and August, J. T. (1993) *J. Biol. Chem.* **268,** 1941–1946
45. Honing, S., Griffith, J., Geuze, H. J., and Hunziker, W. (1996) *EMBO J.* **15,** 5230–5239
46. Ohno, H., Fournier, M. C., Poy, G., and Bonifacino, J. S. (1996) *J. Biol. Chem.* **271,** 29009–29015
47. Harter, C., and Mellman, I. (1992) *J. Cell Biol.* **117,** 311–325

Identification of a Tyrosine-based Motif (YGSI) in the Amino Terminus of Nramp1 (Slc11a1) That Is Important for Lysosomal Targeting

Steven Lam-Yuk-Tseung, Virginie Picard and Philippe Gros

J. Biol. Chem. 2006, 281:31677-31688.
doi: 10.1074/jbc.M601828200 originally published online August 12, 2006
